

Detection of non-Gaussian Fluctuations in a Quantum Point Contact

G. Gershon^a, Yu. Bomze^{a,b}, E. V. Sukhorukov^c, and M. Reznikov^a

^a Department of Physics and Solid State Institute, Technion-IIT, Haifa 32000, Israel

^b Physics Department, Duke University, Durham, NC 27708

^c Département de Physique Théorique, Université de Genève, CH-1211 Genève 4, Switzerland

An experimental study of current fluctuations through a tunable transmission barrier, a quantum point contact, are reported. We measure the probability distribution function of transmitted charge with precision sufficient to extract the first three cumulants. To obtain the intrinsic quantities, corresponding to voltage-biased barrier, we employ a procedure that accounts for the response of the external circuit and the amplifier. The third cumulant, obtained with a high precision, is found to agree with the prediction for the statistics of transport in the non-Poissonian regime.

Recently, measurements of current fluctuations arising from charge discreteness have become an invaluable tool in mesoscopic physics, the most noticeable achievement being the shot noise measurement of quasi-particle charge in the fractional quantum Hall effect [1, 2]. Typically, mesoscopic shot noise experiments report zero-frequency noise power, but this quantity contains only partial information about the statistics of the transmitted charge. The counting statistics (CS) [3] is entirely characterized by the set of cumulants (irreducible moments) $\langle\langle q^n \rangle\rangle$ of the charge $q(\tau)$ transmitted through a voltage-biased system during a sampling time τ . In the long time limit they are proportional to the time, $\langle\langle q^n \rangle\rangle = \langle\langle J^n \rangle\rangle \tau$; this expression defines the *current cumulants* $\langle\langle J^n \rangle\rangle$. For example, Gaussian noise is fully determined by the first two current cumulants, the average current $I = \langle\langle J \rangle\rangle$ and the noise power $S = \langle\langle J^2 \rangle\rangle$. The simplest measure of the non-Gaussianity, the third current cumulant $S = \langle\langle J^3 \rangle\rangle$ which reflects the skewness of the current distribution, is the central focus of our paper. It is linear and universal at low bias voltage, and therefore may be used as a tool for investigation of strongly correlated systems, where large bias cannot be applied without substantially affecting their properties.

However, during a typical sampling time a large number of electrons passes through the system. This fact, by virtue of the central limit theorem, makes it difficult to observe non-Gaussian effects in electron transport [4], unless electrons are counted one by one as, e. g., in Coulomb blockaded quantum dots [6, 7, 8]. To date, $\langle\langle J^3 \rangle\rangle$ has been measured only in low transmission tunneling junctions either by measuring voltage on a load resistor [9, 10], or with the help of the on-chip Josephson threshold detector [11].

In a typical experiment, due to the electrons' charge, the voltage across the sample is not constant, so the measured statistics are not trivially related to the CS of the voltage-biased system. Indeed, the original experiment on the third cumulant of a tunneling current [9] exhibited totally unexpected results, which were explained [12, 13, 14, 15] by the back-action of the measurement apparatus on the sample. That is, in addition

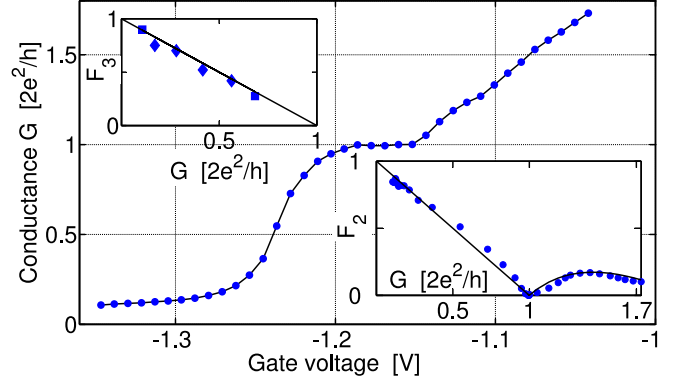


FIG. 1: The conductance step of $g_0 = 2e^2/h$ versus gate voltage V_g used to control the transmission Γ of QPC conduction channels is shown for one of our samples. Lower inset: The Fano factor $F_2 = S/eI$ versus the QPC conductance G/g_0 for the same sample. Solid line is the theoretical prediction, Eq. (7), for the large bias, $eV \gg k_B T$ ($T = 1.8$ K, $B = 2.2$ T). Upper inset: The Fano factor $F_3 = \langle\langle J^3 \rangle\rangle / e^2 I$ versus Γ at low bias, $eV \ll k_B T$ ($T \approx 5$ K), for QPC1 (\blacklozenge), and QPC2 (\blacksquare). Theoretical prediction $F_3 = (1 - \Gamma)$ is shown by the solid line.

to $\langle\langle J^3 \rangle\rangle$, the experimentally measured potential fluctuations also contain contributions, dubbed “cascade corrections” in Ref. [13], from the voltage dependent current I and noise power S . Surprisingly, even if the load resistance is small, the cascade corrections may be of the same order as $\langle\langle J^3 \rangle\rangle$.

We report here the first measurement of the third cumulant of the *non-Poissonian* current partitioned by a variable transmission barrier. To obtain the third cumulant, we develop a procedure that allows us to separate the $\langle\langle J^3 \rangle\rangle$ contribution and cascade corrections in a reliable fashion. In particular, the frequency dependence of the amplifier gain is found to affect these contributions differently. The resulting cumulant $\langle\langle J^3 \rangle\rangle$ agrees accurately with the predictions of [3] for all transmissions, $0 < \Gamma < 1$, without fitting parameters. As a variable transmission barrier we use a quantum point contact (QPC) – a small quasi-1D constriction formed in a 2D electron gas by negative voltage V_g applied to split gates [16]. By varying V_g one can gradually in-

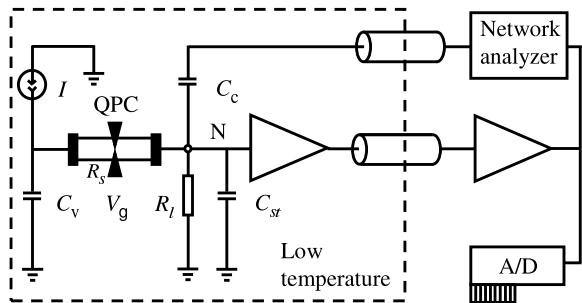


FIG. 2: Experimental setup schematic. The current source drives constant *average* current I through the QPC sample, while the capacitor C_V fixes the voltage across the sample. The QPC resistance R_s can be tuned by the gate voltage V_g . R_l is the load resistance and C_{st} is the stray capacitance of the wires at the amplifier input (the point N). Current fluctuations generate voltage fluctuations at the point N, which are amplified and digitized by 12 bit analog-to-digital convertor (A/D). We introduce current through the capacitor C_c and measure the response with a network analyzer to calibrate the setup.

crease the width of the constriction. Fig. 1 shows a typical dependence of the QPC conductance on V_g . The $g_0 = 2e^2/h$ step in conductance vs. V_g , and the accompanying noise minimum (bottom inset), defines the lowest spin-degenerate QPC channel used in this work. We define the average QPC transmission as:

$$\Gamma(I) = \frac{I}{g_0 V_s(I)}, \quad (1)$$

where I is the average current and V_s is the voltage across the sample. The observed noise agrees well with the theoretical expectations [17] and has only thermal and shot noise contributions. No material contribution, e.g. $1/f$ noise, is detected. The measurements are done at elevated temperature $T \approx 5$ K in order to reduce nonlinearity of the current-voltage characteristic. Nevertheless, for QPC conductance below $2e^2/h$, the transport is dominated by a single channel, as confirmed by the agreement of the measured noise with the single-channel expectations (see Fig. 3).

It is instructive to discuss the issues encountered in the investigation of the third cumulant prior to presenting our experimental results. We focus on the experimental setup shown in Fig. 2, however our conclusions are quite general. Current fluctuations J generated by the QPC sample and by thermal noise in the load resistor R_l give rise to the voltage $V_N(\omega) = Z(\omega)J(\omega)$ at the amplifier input (point N in Fig. 2), where the impedance $Z(\omega) = R_{||}/(1 - i\omega\tau_{RC})$ is determined by $R_{||} = R_s R_l / (R_s + R_l) \approx 7$ KOhm, and by the time constant $\tau_{RC} = R_{||} C_{||}$ (here $C_{||} = C_{st} + C_c \approx 3$ pf) which sets the high frequency cut-off of the circuit $1/(2\pi\tau_{RC}) \approx 7$ MHz. The amplified voltage is:

$$V_a(\omega) = K(\omega)V_N = A(\omega)J(\omega), \quad (2)$$

where K is the amplifier gain and V_N is the input voltage.

In the long time limit (which is justified since the high frequency cut-off of the system is much smaller than $\max(eV_s, k_B T)/h$) all current cumulants are frequency-independent. The amplified voltage fluctuations $\langle\langle V_a^2 \rangle\rangle = \langle\langle [\delta V_a(t)]^2 \rangle\rangle$ bear a simple relation to the noise power $S = \langle\langle J^2 \rangle\rangle$ [18]:

$$\langle\langle V_a^2 \rangle\rangle = B_2 S, \quad B_2 = \frac{1}{2\pi} \int_{-\infty}^{+\infty} A(\omega)A(-\omega)d\omega. \quad (3)$$

In contrast, the third cumulant $\langle\langle V_a^3 \rangle\rangle = \langle\langle [\delta V_a(t)]^3 \rangle\rangle$, may be decomposed as

$$\langle\langle V_a^3 \rangle\rangle = B_3 \langle\langle J^3 \rangle\rangle + B_{en} \mathcal{J}_{en} + B_{nl} \mathcal{J}_{nl} \quad (4)$$

That is, apart the third current cumulant $\langle\langle J^3 \rangle\rangle$, it also contains “environmental” cascade correction \mathcal{J}_{en} originating from the back-action of the voltage fluctuation across the load on the current fluctuations in the sample at later times [12, 13, 14, 15], and the correction \mathcal{J}_{nl} due to nonlinearity of the sample:

$$\mathcal{J}_{en} = 3R_{||} S dS/dV_N \quad (5)$$

$$\mathcal{J}_{nl} = 3R_{||}^2 S^2 d^2 I/d^2 V_N, \quad (6)$$

where $S = S_s + S_l$ is the noise power generated by the sample and the load. The coefficients B_3 , B_{en} , B_{nl} , derived below, depend on the circuit only and are of the same order. The thermal noise of the load and its resistance are current-independent, and thus do not contribute to the derivative. Note that since $R_{||} S \rightarrow 2k_B T$ at $R_{||} \rightarrow 0$, reducing load resistance does not eliminate the corrections (5) and (6).

Our measurements are performed using a setup (see Fig. 2) similar to the one discussed in detail in [10]. We improved it by increasing the total gain of the amplification chain to utilize the full 12 bit resolution of the A/D converter, thus eliminating the necessity to compensate for its nonlinearity. We also managed to reduce the nonlinearity of the cryogenic amplifier by increasing the current through the transistors. The amplified signal is computer analyzed to construct the probability distribution function (PDF) of the amplified voltage (2). We calibrate the setup by introducing a known ac signal, spanning the entire frequency band of the amplifier, through a small capacitor $C_c \approx 2.4$ pF. This gives us the complex-valued $A(\omega)$ [see Eq. (2)] independently at each value I and V_g , which is subsequently used to compute the coefficients in Eqs. (3) and (4).

To compensate for inaccuracy in the calibration and for the drift of amplifier parameters we multiply the measured $A(\omega)$ by a numerical factor, which scales the measured noise S to the theoretical prediction [17]

$$S = eI \left[(1 - \Gamma) \coth \left(\frac{U}{2} \right) + \frac{2\Gamma}{U} \right], \quad U \equiv \frac{eV_s}{k_B T}. \quad (7)$$

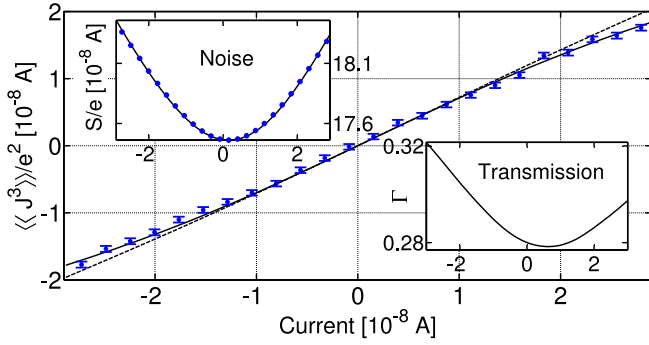


FIG. 3: The current cumulant $\langle\langle J^3 \rangle\rangle$ at $\Gamma \sim 0.3$, derived from the experimental results for $\langle\langle V_a^2 \rangle\rangle$ and $\langle\langle V_a^3 \rangle\rangle$ using Eq. (4-6) for the sample QPC2 measured with amplifier *b*. Solid line is the theoretical prediction for $\langle\langle J^3 \rangle\rangle$, Eq. (8); the dashed line is the low-bias limit, Eq. (9), with current-dependent transmission Γ (lower inset). Upper inset: Measured value of the noise power S versus current; solid line is the Eq. (7).

This scale, determined individually for each value of V_g , is found to deviate from unity by less than 10%. This is illustrated in the upper inset of Fig. 3, which shows S fitted by Eq. (7) at V_g corresponding to the transmission $\Gamma \approx 0.3$ (see the lower inset of Fig. 3). We use the scaled $A(\omega)$ to find the coefficients B_3 , B_{en} , B_{nl} , and then to obtain $\langle\langle J^3 \rangle\rangle$ from Eqs. (4) and (5). The resulting $\langle\langle J^3 \rangle\rangle$ is shown in the main panel of Fig. 3.

As seen in Fig. 3, the measured third current cumulant $\langle\langle J^3 \rangle\rangle$ shows very good agreement with the prediction for noninteracting fermions [3, 5]:

$$\langle\langle J^3 \rangle\rangle = e^2 I (1 - \Gamma) \left[\frac{6\Gamma \sinh(U) - U}{U \cosh(U) - 1} + 1 - 2\Gamma \right]. \quad (8)$$

Although the procedure that leads to $\langle\langle J^3 \rangle\rangle$ involves subtraction of several terms of comparable magnitude, we stress that it does not rely on any fitting parameter other than the aforementioned scaling factor. Since we observe no systematic deviation from the prediction (8), we believe that the main sources of error in our experiment are statistical fluctuations (indicated by error bars in Fig. 3), as well as our lack of knowledge of the precise energy dependence of Γ .

The nearly linear behavior of $\langle\langle J^3 \rangle\rangle$ at $I \leq 10$ nA corresponds to the low-bias limit of Eq. (8):

$$\langle\langle J^3 \rangle\rangle = e^2 I (1 - \Gamma), \quad |U| \ll 1. \quad (9)$$

The dashed line in Fig. 3 shows the prediction (9) with the measured current-dependent transmission $\Gamma(I)$. Notably, the full expression (8) provides a much better fit to our data than the low-bias limit (9). In the data taken at larger bias (see Fig. 4), for which the quantity U could be as large as 4, the agreement with the expression (8) remains very good. We also note that the large bias limit of Eq. (8), $\langle\langle J^3 \rangle\rangle = e^2 I (1 - \Gamma)(1 - 2\Gamma)$, exhibits a sign change at $\Gamma = 1/2$. However, the bias regime needed

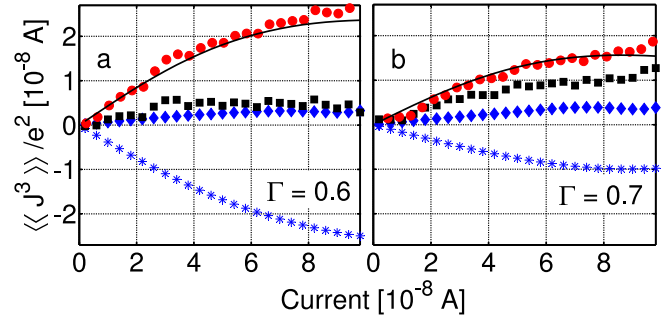


FIG. 4: The contributions used to evaluate $\langle\langle J^3 \rangle\rangle$ (\bullet) from Eqs. (4-6): $\langle\langle V_a^3 \rangle\rangle/B_3$ (\blacksquare), $\mathcal{J}_{\text{en}} B_{\text{en}}/B_3$ ($*$), and $\mathcal{J}_{\text{nl}} B_{\text{nl}}/B_3$ (\blacklozenge). Panels (a) and (b) show the results obtained with two different amplifiers, *a* and *b*, on the sample QPC1 for similar transmissions $\Gamma = 0.6$ and 0.7 . The coefficients B_3 , B_{en} , and B_{nl} are calculated using measured response function $A(\omega)$. Solid line is the prediction (8).

to observe this effect, $U \gtrsim 10$, is not accessible in our experiment because of the nonlinearity in $I(V_S)$.

In this work we present the data obtained on two different samples, QPC1 and QPC2. The sample QPC1 is measured with two amplifiers, *a* and *b*, which have different low frequency cut-offs, $\nu_{<}^{(a)} \approx 300$ KHz and $\nu_{<}^{(b)} \approx 4$ MHz, and upper cut-off frequency $\nu_{>} \gg 1/(2\pi\tau_{RC}) \approx 7$ MHz. For comparison, we show the results for two similar QPC transmissions in Fig. 4. Although the contributions to $\langle\langle J^3 \rangle\rangle$ are quite different, the resulting current cumulants are close and agree well with the theory. This underscores the necessity of accounting for the frequency dependent amplifier gain $A(\omega)$ in data processing. The low bias results for two different samples are summarized in the upper inset of Fig. 1: the slope of the $\langle\langle J^3 \rangle\rangle$ vs. current, the Fano factor $F_3 = \langle\langle J^3 \rangle\rangle/e^2 I$ is proportional to $(1 - \Gamma)$, confirming universality of the relation (9).

In the rest of the paper we derive B_{en} and B_{nl} , and express them through $A(\omega)$ and the input circuit parameters. Fluctuations are treated in the time domain using the Fourier transforms $A(t)$, $Z(t)$, and $K(t)$, which vanish for $t < 0$ due to causality. The fluctuation $V(t) = V_N - IR_l$ of the voltage $V_N(t)$ is generated by the current noise J according to

$$C_{\parallel} \dot{V} = -R_{\parallel}^{-1} V + \frac{d^2 I}{dV_N^2} \frac{V^2}{2} + J. \quad (10)$$

Solving linearized equation (10) yields an exponential relaxation of fluctuations:

$$V(t) = \int dt_1 Z(t - t_1) J(t_1), \quad (11)$$

where $Z(t) = C_{\parallel}^{-1} e^{-t/\tau_{RC}}$. The amplified voltage V_a is related to $V(t)$ as:

$$V_a(t) = \int dt' K(t - t') V(t') = \int dt_1 A(t - t_1) J(t_1).$$

We next ensemble-average the value $[V_a(t) - \langle V_a \rangle]^3$. The intrinsic contribution arises from $\langle\langle J(t_1)J(t_2)J(t_3) \rangle\rangle$, where $J(t)$ can be treated as δ -correlated in time. This leads to the first term in Eq. (4) with B_3 given by [19]:

$$B_3 = \frac{1}{(2\pi)^2} \iint_{-\infty}^{+\infty} A(\omega)A(\omega')A(-\omega - \omega')d\omega d\omega' \quad (12)$$

The voltage across the sample fluctuates in time, being a function of current fluctuations at preceding times, as described by (11). As a result, the average $\langle J(t_1)J(t_2)J(t_3) \rangle$ contains the environmental contribution due to the dependence of the correlator

$$\langle\langle J(t_1)J(t_2) \rangle\rangle = \delta(t_1 - t_2)S(V) \quad (13)$$

on the voltage V , which in turn depends on the current J at an earlier time t' . Linear in V expansion of Eq. (13) gives the environmental contribution to Eq. (4):

$$\begin{aligned} & 3 \int dt_1 A^2(-t_1) \frac{dS}{dV_N} \int dt' Z(t_1 - t') \\ & \times \langle\langle J(t') \int dt_3 A(-t_3)J(t_3) \rangle\rangle = 3R_{\parallel} S \frac{dS}{dV_N} B_{\text{en}}, \\ B_{\text{en}} & = R_{\parallel}^{-1} \int dt_1 A^2(-t_1) \int dt_3 Z(t_1 - t_3)A(-t_3), \end{aligned} \quad (14)$$

where the factor 3 accounts for the three possibilities to choose a later time.

Finally, the nonlinear contribution to Eq. (4) comes from the V^2 term in Eq. (10) with the coefficient

$$B_{\text{nl}} = R_{\parallel}^{-2} \int dt A(-t) \left(\int dt_1 A(-t_1)Z(t - t_1) \right)^2. \quad (15)$$

For the frequency independent amplification K , we find:

$$B_3 = 2B_{\text{en}} = 4B_{\text{nl}} = K^3 \tau_{RC} / 3C^3. \quad (16)$$

In this case, the first two terms in Eq. (4) cancel at small I and R_l . Our amplifier a , having $\nu_{<} \approx 300$ KHz, operates close to this regime (see Fig. 4).

It is instructive to note that the ratio of the intrinsic and environmental coefficients in Eq. (16) is twice as large as that of Refs. [12, 13, 14, 15]. This difference can be traced to different assumptions about frequency dependence of the system gain. Refs. [12, 13, 14, 15] focus on the limit of the high frequency cutoff set by the amplifier, while in Eq. (16), as well as in our experiment, it is determined by $Z(\omega)$ with the roll-off set by $1/\tau_{RC}$. Therefore, our results correspond to the equal time correlator $\langle\langle V^3 \rangle\rangle = \langle[\delta V(t)]^3\rangle$.

In summary, we have measured the third cumulant of shot noise in variable transmission QPCs in the essentially non-Poissonian regime. In order to extract the ‘‘intrinsic’’ third current cumulant we developed a technique which allows reliable subtraction of the environmental and nonlinear circuit-dependent contributions. Good agreement between the experimental results and the expectations, Ref. [3], opens a venue for using high order cumulants as an experimental tool in mesoscopic physics.

We thank L. Levitov for valuable discussions, D. Goldhaber-Gordon for providing GaAs wafers, and D. Shovkun for his contributions at early stages of this work. This research was supported by the US-Israel Binational Science Foundation, Israel Science Foundation, Lady Davis Fellowship, and Swiss NSF.

- [1] L. Saminadayar *et al.*, Phys. Rev. Lett. **79**, 2526 (1997); R. de Picciotto *et al.*, Nature (London) **389**, 162 (1997).
- [2] M. Reznikov *et al.*, Nature (London) **399**, 238 (1999).
- [3] L.S. Levitov, G.B. Lesovik, JETP Lett. **58**, 230 (1993); cond-mat/9401004
- [4] According to Ref. [5], it is progressively difficult to extract high order current cumulants from the probability distribution of transmitted charge, because the signal-to-noise ratio scales as $(e/q)^{n/2-1}$.
- [5] L.S. Levitov, M. Reznikov, Phys. Rev. B **70**, 115305 (2004).
- [6] T. Fujisawa *et al.*, Science **312**, 1634 (2006).
- [7] S. Gustavsson *et al.*, Phys. Rev. Lett. **96**, 076605 (2006).
- [8] S. Gustavsson *et al.*, Phys. Rev. B **75**, 075314 (2007).
- [9] B. Reulet, J. Senzier and D.E. Prober, Phys. Rev. Lett. **91**, 196601 (2003).
- [10] Yu. Bomze *et al.*, Phys. Rev. Lett. **95**, 176601 (2005).
- [11] A.V. Timofeev *et al.*, Phys. Rev. Lett. **98**, 207001 (2007).
- [12] M. Kindermann, Yu.V. Nazarov, C.W.J. Beenakker Phys. Rev. Lett. **90**, 246805 (2003).
- [13] K.E. Nagaev, Phys. Rev. B **66**, 075334 (2002).
- [14] C.W.J. Beenakker, M. Kindermann, and Yu.V. Nazarov, Phys. Rev. Lett. **90**, 176802 (2003).
- [15] S. Pilgram *et al.*, Phys. Rev. Lett. **90**, 206801 (2003); A.N. Jordan, E.V. Sukhorukov, S. Pilgram, J. Math. Phys. **45**, 4386 (2004).
- [16] B.J. van Wees *et al.*, Phys. Rev. Lett. **60**, 848 (1988); D.A. Wharam *et al.*, J. Phys. C **21**, L209 (1988).
- [17] Ya. M. Blanter and M. Büttiker, Physics Reports **336**, 1-166 (2000).
- [18] Our definition of noise moments differs by a factor of 2 from the one based on the positive frequency representation for the noise power spectrum, which brings the Schottky relation to the form $S = eI$.
- [19] B. Reulet *et al.*, Proceedings of SPIE, Fluctuations and Noise in Materials , 5469-33:244-56 (2004); cond-mat/0403437.